ELSEVIER

Journal of Organometallic Chemistry 637–639 (2001) 167–171

Journal of Organometallic Chemistry

www.elsevier.com/locate/jorganchem

# Iron(II) versus osmium(II) oxidation in 1,1′-bis(diorganophosphino)ferrocene–osmium(II) complexes

Wolfgang Kaim [a,*], Torsten Sixt [a], Michael Weber [a], Jan Fiedler [b]

[a] *Institut für Anorganische Chemie, Universität Stuttgart, Pfaffenwaldring 55, D-70550 Stuttgart, Germany*

[b] *J. Heyrovsky Institute of Physical Chemistry, Academy of Sciences of the Czech Republic, Dolejškova 3, CZ-18223 Prague, Czech Republic*

Received 18 December 2000; received in revised form 14 March 2001; accepted 23 March 2001

**Abstract**

The compounds $[(Cym)OsCl(dxpf)](PF_6)$, Cym = *p*-cymene and dxpf: 1,1′-bis(diphenylphosphino)ferrocene (dppf), 1,1′-bis(diethylphosphino)ferrocene (depf) or 1,1′-bis(diisopropylphosphino)ferrocene (dippf), were synthesized and characterized by NMR ($^1H$, $^{31}P$) and, in the case of $[(Cym)OsCl(dppf)](PF_6)$, by X-ray structure analysis of the acetonitrile solvate. EPR and UV–vis spectroelectrochemistry indicate the formation of an osmium(II)–ferrocenium species on reversible one-electron oxidation. The second oxidation and the reduction are electrochemically irreversible. 

*Keywords:* Crystal structures; Electrochemistry; EPR spectroscopy; Ferrocene compounds; Osmium complexes

## 1. Introduction

Reversible formation of the ferrocenium state at rather low potentials has been one of the most characteristic elementary reactions of the ferrocene [1] moiety in mononuclear or oligonuclear systems [2–4]. When coupled to a similarly oxidizable metal center M [5] the question arises whether the ferrocene iron or M is oxidized first. Using 1,1′-bis(diphenylphosphino)-ferrocene (dppf) as a chelating ligand for organoruthenium complex fragments we could recently show by EPR and UV–vis spectroscopy that $[(\eta^5\text{-}C_5Me_5)\text{-}RuH(dppf)]$ is oxidized to a ferrocene–ruthenium(III) state whereas $[(\eta^6\text{-}Cym)RuCl(dppf)]^+$, Cym = *p*-cymene = 1-isopropyl-4-methylbenzene, forms a ferrocenium–ruthenium(II) species [5]. Both systems are of interest as catalyst models for hydrogenase enzymes and fuel cell reactions such as $H_2 \rightarrow 2e^- + 2H^+$ [6,7].

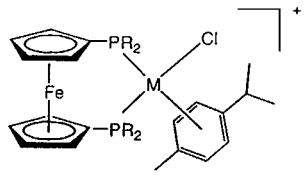


Replacing ruthenium(II) with the generally better oxidizable [8,9] osmium(II) in compounds $[(Cym)OsCl(dxpf)](PF_6)$, dxpf = dppf, 1,1′-bis(diethylphosphino)ferrocene (depf) or 1,1′-bis(diisopropylphosphino)ferrocene (dippf) [10], we set out to study whether the ferrocene–osmium(III) or ferrocenium–osmium(II) formulation is valid for the electrogenerated ions $[(Cym)OsCl(dxpf)]^{2+}$. Cyclic voltammetry, supported by spectroelectrochemistry (UV–vis, EPR), can be expected to provide an unambiguous distinction between both the alternatives [5].

## 2. Results and discussion

### 2.1. Synthesis and NMR spectroscopy

The heterobimetallic complexes $[(Cym)OsCl(dxpf)](PF_6)$ were obtained from the precursors dxpf and

* Corresponding author. Tel.: +49-711-685-4170/71; fax: +49-711-685-4165.

*E-mail address:* kaim@iac.uni-stuttgart.de (W. Kaim).

0022-328X/01/$ - see front matter 
PII: S0022-328X(01)00898-1

Table 1
$^1$H- and $^{31}$P-NMR chemical shifts of complexes in $(CD_3)_2CO$

| Compound | $\delta$ ($^1$H) | | | | | | $\delta$ ($^{31}$P) [a] |
|---|---|---|---|---|---|---|---|
| | CH (Fc) | | | | CH (Cym) | $CH_3$ (Me/$^i$Pr) | |
| [CymOsCl(dppf)]($PF_6$) | 4.17 | 4.33 | 4.46 | 5.07 | 5.82/5.32 | 1.16/0.89 | −11.90 |
| [CymOsCl(depf)]($PF_6$) | 4.31 | 4.47 | 4.61 | 4.83 | 6.03/6.53 | 2.42/1.35 | −16.21 |
| [CymOsCl(dippf)]($PF_6$) | 4.28 | 4.48 | 4.54 | 4.89 | 7.11/6.10 | 2.64/1.34 | −5.15 |
| [CymRuCl(dppf)]($PF_6$) | 4.20 | 4.39 | 4.48 | 5.05 | 5.75/5.52 | 1.04/0.87 | 37.15 |

[a] Phosphoric acid standard.

[(Cym)$OsCl_2$] [11] through activation with $TlNO_3$ (depf, dippf) or $Cl^-/PF_6^-$ ion exchange after thermal activation (dppf). Without chemical or thermal activation, neutral trinuclear complexes {(μ-dxpf)[(Cym)$OsCl_2]_2$} are formed which will be described separately [7].

$^1$H- and $^{31}$P-NMR data confirm the symmetrical coordination of the dxpf ligands by osmium (Table 1), they also illustrate the better π back donation to $^{31}$P nuclei from osmium(II) in comparison to ruthenium(II) and the mobility of the Cym decks (broadened $^1$H resonances). As the structure analysis confirms (cf. below), the distinct low-field shift among some ferrocenyl protons is related to interaction with the chloride centers.

Table 2
Crystallographic data and refinement parameters of [(Cym)OsCl(dppf)]($PF_6$)·$CH_3CN$

| | |
|---|---|
| Empirical formula | $C_{46}H_{45}ClF_6FeNOsP_3$ |
| Formula weight | 1100.24 |
| Crystal size (mm) | 0.4 × 0.35 × 0.2 |
| Temperature (K) | 173 |
| Crystal system | Monoclinic |
| Space group | $P2_1/c$ |
| Unit cell dimensions | |
| $a$ (Å) | 11.384(2) |
| $b$ (Å) | 18.417(3) |
| $c$ (Å) | 20.545(4) |
| $\beta$ (°) | 90.017(14) |
| $V$ (Å$^3$) | 4307.4(12) |
| $Z$ | 4 |
| $D_{calc}$ (g cm$^{-3}$) | 1.697 |
| Absorption coefficient (mm$^{-1}$) | 3.518 |
| 2$\theta$ Range (°) | 1.79–29.99 |
| Index ranges | $-1 \le h \le 16$, $-9 \le k \le 25$, $-11 \le l \le 28$ |
| Reflections collected | 8253 |
| Number of unique reflections | 7516 |
| Goodness-of-fit on $F^2$ [a] | 1.026 |
| Data/restraints/parameters | 7511/0/533 |
| $R[I > 2\sigma(I)]$ | $R_1 = 0.0398$, $R_w = 0.0828$ |
| $R$ indices (all data) [b,c] | $R_1 = 0.0659$, $R_w = 0.0956$ |
| Largest residual density (e Å$^{-3}$) | 0.810 and −0.490 |

The structure was obtained on a Siemens four-circle diffractometer P4, graphite monochromate Mo–$K_\alpha$ radiation ($\lambda = 0.71073$ Å).

[a] Goodness-of-fit = $\{\Sigma w(|F_o|^2 - |F_c|^2)^2/(n-m)\}^{1/2}$ where $n$ = number of data and $m$ = number of variables.

[b] $R_1 = (\Sigma||F_o| - |F_c||)/\Sigma|F_o|$.

[c] $R_w = \{\Sigma[w(|F_o|^2 - |F_c|^2)^2]/\Sigma[w|F_o|^4]\}^{1/2}$.

## 2.2. Structure of [(Cym)OsCl(dppf)]($PF_6$)·$CH_3CN$

Crystals of the dppf complex salt could be obtained from acetonitrile. The results of the structural analysis are summarized and illustrated in Table 2 and in Fig. 1.

The structure of the dppf complex cation is similar to that of the analogous [(Cym)RuCl(dppf)]$^+$ as reported by Jensen et al. [12a] from [(Cym)RuCl(dppf)]($PF_6$) and as determined by us for [(Cym)RuCl(dppf)]-($PF_6$)·0.5$CH_3OH$ [7]. Similar ruthenium systems with alkylated arene ligands were described by Mai and Yamamoto [12b]. In this variant of a 'piano stool' arrangement the *p*-cymene 'deck' exhibits slight distortion toward a boat conformation with the bulky isopropyl substituent oriented away from the side of the chloride ligand at the osmium center; the P–Os–P angle is larger at 95.02(8)° than the P–Os–Cl angles (< 87°). As expected, the Os–E bond lengths are similar to corresponding Ru–E distances [7,12]. Remarkably, the $C_5H_4$ decks of the ferrocene moiety are almost fully eclipsed [1] with a twist angle of only 4.6°. This confor-

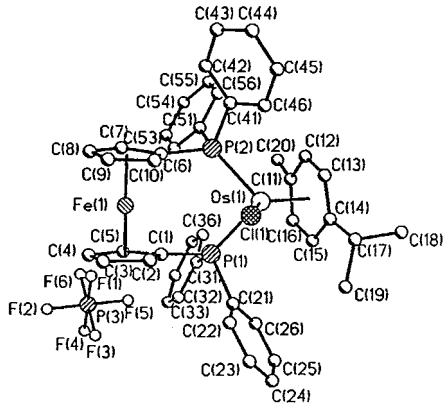


Fig. 1. Structure of [(Cym)OsCl(dppf)]($PF_6$)·$CH_3CN$ in the crystal. Selected distances (Å) and angles (°): Os–P(1), 2.352(2); Os–P(2), 2.377(2); Os–Cl, 2.408(2); Os–Fe, 4.504(1). Cl–Os–P(1), 82.99(7); Cl–Os–P(2), 86.96(7); P(1)–Os–P(2), 95.02(8).

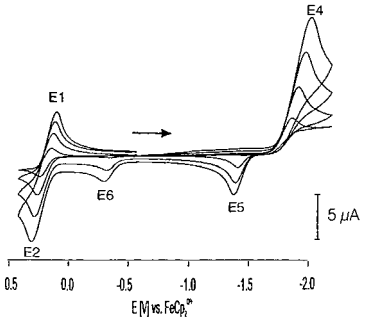


Fig. 2. Cyclic voltammetry of [(Cym)OsCl(dippf)]($PF_6$) in THF/0.1 M $Bu_4NPF_6$ at scan rates of 250, 100, 50 and 25 mV $s^{-1}$.

mation of the complex cation may be related to one rather short Cl···H($C_5H_4$) contact of 292.8 pm which also explains the low-field shift of ferrocenyl protons in the $^1$H-NMR spectra (Table 1).

### 2.3. Cyclic voltammetry

A typical cyclic voltammogram of the complexes [(Cym)OsCl(dxpf)]($PF_6$) is shown in Fig. 2, illustrating the effect of variable scan rate. Table 3 summarizes the electrochemical data which were obtained in THF solution.

The heterodinuclear complexes are oxidized reversibly in a one-electron step $E_2/E_1$; further, irreversible oxidation occurs at anodic peak potentials $E_3$ about 1 V higher than $E_2$. The rather large peak potential differences of about 100 mV for $E_2/E_1$ indicate some conformational change after oxidation. There is very little difference between the corresponding osmium and ruthenium complexes of dppf [5], suggesting already a primary oxidation of the ferrocene iron center. Thus, formation of a ferrocenium–osmium(II) intermediate occurs prior to the irreversible oxidation to an osmium(III) species which exists only at rather high potentials $E_3 > 1$ V, in agreement with literature values [8]. The half-wave potentials $E_2/E_1$ for the 1,1′-bis(diorganophosphino)ferrocene/ferrocenium oxidation also reflect the influence of the substituents at the phosphorus atoms, viz., slightly facilitated oxidation with the more electron donating alkyl groups.

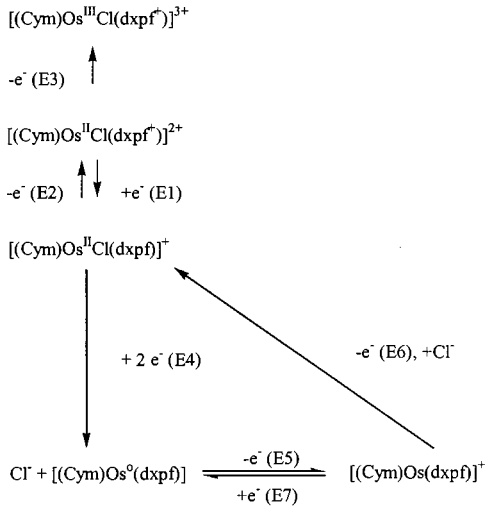


Scheme 1.

In analogy to complexes of α-diimines with arenechloroosmium(II) fragments [8,13] the cations [(Cym)OsCl(dxpf)]$^+$ are reduced irreversibly in a two-electron step at peak potential $E_4$ with the loss of the halide ligand and formation of [(Cym)Os(dxpf)] (EEC or ECE mechanism [8,13,14]). In comparison to [(Cym)OsCl(bpy)]$^+$, bpy = 2,2′-bipyridine [8], these cathodic peak potentials are shifted by about 0.5 V toward more negative values which demonstrates the less pronounced π acceptor capability of the dxpf ligands. The intensities of the reoxidation peaks at $E_5$ and $E_6$ depend on the scan rate as shown in Fig. 2, illustrating the slow association of chloride. Scheme 1 summarizes the reactions which occur in the cyclic voltammetric experiments.

### 2.4. UV–vis spectroelectrochemistry

The electrochemically reversible oxidation of the complexes [(Cym)OsCl(dxpf)]($PF_6$), dxpf = dppf and

Table 3
Electrochemical data of complexes [a]

| Complex cation | $E_1/E_2$ [b] | $E_3$ [c] | $E_4$ [d] | $E_5$ [c] | $E_6$ [c] |
|---|---|---|---|---|---|
| [(Cym)OsCl(dppf)]$^+$ | 0.39 | 1.27 | −1.96 | −1.04 | −0.06 |
| [(Cym)OsCl(depf)]$^+$ | 0.36 | [e] | −2.09 | [e] | [e] |
| [(Cym)OsCl(dippf)]$^+$ | 0.27 | 1.34 | −1.85 | −1.31 [f] | −0.28 |
| [(Cym)RuCl(dppf)]$^+$ | 0.38 | 1.25 | −1.74 | −1.11 | 0.44 |

[a] From cyclic voltammetry at 100 mV $s^{-1}$ in THF/0.1 M $Bu_4NPF_6$, potentials in V vs. ferrocene/ferrocenium.
[b] Half-wave potential ($\Delta E_{pp} \approx 100$ mV).
[c] Anodic peak potentials.
[d] Cathodic peak potentials for irreversible two-electron process.
[e] Not observed.
[f] $E_7$ at −1.44 V.

dippf, was studied via an optically transparent thin-layer electrolytic (OTTLE) cell [15] in the UV–vis region. The characteristic feature as illustrated in Fig. 3 is the emergence of weak absorption bands at 648 nm (dppf) or 631 nm (dippf), respectively, on oxidation. This absorption is attributed to the typical LMCT transition $^2e_{2g} \rightarrow {}^2e_{1u}$ of the ferrocenium chromophore [16,17]. Absorptions involving osmium(III) are expected to occur at longer wavelengths due to singlet–triplet transitions which become allowed for systems with high spin–orbit coupling contributions [17,18].

### 2.5. EPR spectroscopy

The EPR spectra of ferrocenium species ($^2e_{2g}$ ground state) are distinguished by a large $g$ anisotropy with $g_1 \approx 4$ and $g_{2,3} < 2$ [19]. In addition, rapid relaxation often causes line broadening which renders the spectra observable only below 50 K [5,19]. The electrogenerated complex dication $[(Cym)OsCl(dppf)]^{2+}$ as studied at 4 K in glassy frozen THF displays essentially the same EPR features ($g_1 = 3.667$, $g_{2,3} = 1.730$) as the ruthenium analogue ($g_1 = 3.512$, $g_{2,3} = 1.765$) which confirms the ferrocenium formulation for this one-electron oxidized form. The slightly larger $g$ anisotropy of the osmium species may reflect marginal contributions from the 5d center with its high spin–orbit coupling constant [17,18].

## 3. Conclusions

It is evident from the results presented here that the replacement of Ru by Os in complexes $[(Cym)MCl(dxpf)]^{2+}$ is not sufficient to switch from a ferrocenium–M(II) to a ferrocene–M(III) state after the loss of one electron. In fact, the differences between both complexes $[(Cym)MCl(dppf)](PF_6)$, M = Ru, Os, are quite marginal, as are the substituent effects at the phosphorus atoms. The most significant differences relate to the slower chemical reactivity of the osmium analogues in electrochemical experiments. Higher electron density at ruthenium and the lower overall charge are obviously crucial for the formation of the ferrocene–ruthenium(III) alternative in the cation $[(C_5Me_5)RuH(dppf)]^+$ [5], variation of the ancillary ligands at M appears to be more effective than the Ru/Os exchange alone.

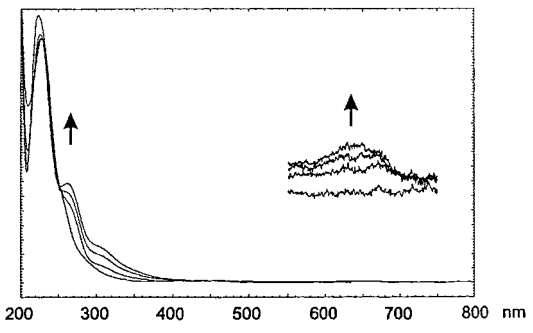


Fig. 3. Absorption spectral changes of $[(Cym)OsCl(dppf)]^{(+)\rightarrow(2+)}$ from UV–vis spectroelectrochemistry in THF/0.1 M $Bu_4NPF_6$.

## 4. Experimental

### 4.1. Syntheses

#### 4.1.1. [(Cym)OsCl(dppf)](PF6)

An amount of 354 mg (0.639 mmol) dppf was added to a suspension of 202 mg (0.256 mmol) $[(Cym)OsCl_2]_2$ [11] in 30 ml MeOH. Heating under reflux for 6 h, addition of 20 ml THF and further heating under reflux for 5 h produced a mixture which was reduced to dryness. Addition of 20 ml MeOH, filtration, reduction of the filtrate to about 5 ml and precipitation with $Et_2O$ gave 470 mg (97%) of the yellow chloride salt. The anion was exchanged by hexafluorophosphate through dissolving in $Me_2CO$ and precipitation with a saturated solution of $Bu_4NPF_6$. Yield: 413 mg (79%). Anal. Found C, 49.78; H, 3.93. Calc. for $C_{44}H_{42}ClF_6FeOsP_3$ (1023.5 g mol$^{-1}$): C, 49.98; H, 4.00%. $^1$H-NMR (acetone-$d_6$): $\delta$ 0.89 (d, 6H, $CH(CH_3)_2$, $^3J = 6.9$ Hz), 1.16 (s, 3H, $CH_3$), 2.60 (sept, 1H, $CH(CH_3)_2$, $^3J = 6.9$ Hz), 4.17 (s, br, Fc–H), 4.33 (s, br, Fc–H), 4.46 (s, br, Fc–H), 5.07 (s, br, Fc–H), 5.60 (d, 2H, Cym, $^3J = 6.0$ Hz), 6.21 (d, 2H, Cym, $^3J = 5.8$ Hz) 7.47–7.76 (m, Ph). $^{31}$P-NMR (acetone-$d_6$): $\delta$ −11.9 ($Fc(PR_2)_2$), −143.55 ($PF_6$).

#### 4.1.2. [(Cym)OsCl(depf)](PF6)

An amount of 174 mg (0.653 mmol) $TlNO_3$ was added to a suspension of 259 mg (0.328 mmol) $[(Cym)OsCl_2]_2$ [11] in 20 ml MeOH–MeCN (1/1). After stirring for 30 min this mixture was added to 248 mg (0.685 mmol) of depf in 30 ml MeOH. After 1 h the volume was reduced and the remaining oily residue taken up with MeOH and reprecipitated as oil by addition of $Et_2O$. Removal of the solvents, dissolution in EtOH–water (4/1) and precipitation with a saturated solution of $NH_4PF_6$ gave a yellow solid which was washed with EtOH–water and then dried under vacuum. Yield: 280 mg (60%). Anal. Found C, 39.27; H, 4.96. Calc. for $C_{28}H_{42}ClF_6FeOsP_3$ (867.05 g mol$^{-1}$): C, 38.79; H, 4.88%. $^1$H-NMR (acetone-$d_6$): $\delta$ 0.96–1.30 (m, 12H, $CH(CH_3)_2$), 1.35 (d, 6H, $CH(CH_3)_2$, $^3J = 6.9$ Hz), 2.08–2.69 (m, 12H, $CH_2CH_3$ and $-CH(CH_3)_2$), 2.42 (s, 3H, $CH_3$), 4.31 (s, br, Fc–H), 4.47 (s, br, Fc–H), 4.61 (s, br, Fc–H), 4.83 (s, br, Fc–H), 6.03 (d, 2H, Cym, $^3J = 6.1$ Hz), 6.53 (d, 2H, Cym, $^3J = 5.8$ Hz). $^{31}$P-NMR (acetone-$d_6$): $\delta$ −16.21 ($Fc(PR_2)_2$), −143.60 ($PF_6$).

#### 4.1.3. [(Cym)OsCl(dippf)](PF6)

Preparation was carried out as described in Section 4.1.2 with 287 mg (0.685 mmol) of dippf. Yellow solid

(342 mg, 73%). Anal. Found: C, 41.68; H, 5.40. Calc. for $C_{32}H_{50}ClF_6FeOsP_3$ (923.16 g mol$^{-1}$): C, 41.63; H, 5.46%. $^1$H-NMR (acetone-$d_6$): $\delta$ 1.13–1.28 (m, 12H, $CH(CH_3)_2$), 1.38 (d, 6H, $CH(CH_3)_2$, $^3J = 6.9$ Hz), 1.40–1.57 (m, 12H, $CH(CH_3)_2$), 2.56 (sept, 4H, $CH(CH_3)_2$, $^3J = 7.0$ Hz), 2.64 (s, 3H, $CH_3$), 4.27 (s, br, Fc–H), 4.48 (s, br, Fc–H), 4.54 (s, br, Fc–H), 4.89 (s, br, Fc–H), 6.10 (d, 2H, Cym, $^3J = 6.1$ Hz), 7.11 (d, 2H, Cym, $^3J = 5.8$ Hz) 7.47–7.76 (m, Ph). $^{31}$P-NMR (acetone-$d_6$): $\delta$ −5.15 ($Fc(PR_2)_2$), −143.54 ($PF_6$).

### 4.2. Instrumentation

EPR spectra were recorded in the X band on a Bruker System ESP 300 equipped with a Bruker ER035M gaussmeter and a HP 5350B microwave counter. $^1$H- and $^{31}$P-NMR spectra were taken on Bruker AC 250 and AC 400 spectrometers. UV–vis absorption spectra were recorded on a Bruins Instruments Omega 10 spectrophotometer. Cyclic voltammetry was carried out in 0.1 M $Bu_4NPF_6$ solutions using a three-electrode configuration (glassy carbon electrode, Pt counter electrode, Ag | AgCl reference) and a PAR 273 potentiostat and function generator. The ferrocene/ferrocenium couple served as an internal reference. Spectroelectrochemical measurements were performed using an OTTLE cell [15] for UV–vis spectra and a two-electrode capillary for EPR studies [20].

### 4.3. Crystallography

Yellow single crystals of [(Cym)OsCl(dppf)]-$(PF_6)\cdot CH_3CN$ were obtained from a saturated solution of the compound in MeCN, cooled to 5 °C. The structure of [(Cym)OsCl(dppf)]$(PF_6)\cdot CH_3CN$ was solved by direct methods. The refinement was carried out employing full-matrix least-squares procedures [21]. All non-hydrogen atoms were refined anisotropically. The hydrogen atoms were introduced at proper geometric positions and treated according to the riding model with isotropic thermal parameters fixed at 20% greater than that of the bonded atom. Anisotropic thermal parameters were refined for all non-hydrogen atoms.

## 5. Supplementary material

Crystallographic data for the structural analysis have been deposited with the Cambridge Crystallographic Data Centre, CCDC no. 151761 for [(Cym)OsCl(dppf)]$(PF_6)\cdot CH_3CN$. Copies of this information may be obtained free of charge from The Director, CCDC, 12 Union Road, Cambridge CB2 1EZ, UK (Fax: +44-1223-336033; e-mail: deposit@ccdc.cam.ac.uk or www: http://www.ccdc.cam.ac.uk).

## Acknowledgements

This work has been supported within the Landesforschungsschwerpunktprogramm Baden-Württemberg, by the Volkswagenstiftung and the Fonds der Chemischen Industrie. We also thank the German–Czech scientific exchange program for support.

## References

[1] T. Togni, T. Hayashi (Eds.), Ferrocenes, VCH, Weinheim, 1995.
[2] D.O. Cowan, R.L. Collins, F. Kaufman, J. Phys. Chem. 75 (1971) 2025.
[3] M. Kurosawa, T. Nankawa, T. Matsuda, K. Kubo, M. Kurihara, H. Nishihara, Inorg. Chem. 38 (1999) 5113.
[4] R. Rulkens, A.J. Lough, I. Manners, S.R. Lovelace, C. Grand, W.E. Geiger, J. Am. Chem. Soc. 118 (1996) 12683.
[5] T. Sixt, J. Fiedler, W. Kaim, Inorg. Chem. Commun. 3 (2000) 80.
[6] R.T. Hembre, J.S. McQueen, V.W. Day, J. Am. Chem. Soc. 118 (1996) 798.
[7] T. Sixt, W. Kaim, unpublished results.
[8] W. Kaim, R. Reinhardt, M. Sieger, Inorg. Chem. 33 (1994) 4453.
[9] W. Kaim, V. Kasack, Inorg. Chem. 29 (1990) 4696.
[10] (a) J.J. Bishop, A. Davison, M.L. Katcher, D.W. Lichtenberg, R.E. Merrill, J.C. Smart, J. Organomet. Chem. 27 (1971) 241; (b) I.R. Butler, W.R. Cullen, T.-J. Kim, Synth. React. Inorg. Met.-Org. Chem. 15 (1985) 109.
[11] H. Werner, K. Zenkert, J. Organomet. Chem. 345 (1988) 151.
[12] (a) S.B. Jensen, S.J. Rodger, M.D. Spicer, J. Organomet. Chem. 556 (1998) 151; (b) J.-F. Mai, Y. Yamamoto, J. Organomet. Chem. 560 (1998) 223.
[13] F. Baumann, A. Stange, W. Kaim, Inorg. Chem. Commun. 1 (1998) 305.
[14] W. Kaim, R. Reinhardt, E. Waldhör, J. Fiedler, J. Organomet. Chem. 524 (1996) 195.
[15] M. Krejcik, M. Danek, F. Hartl, J. Electroanal. Chem. Interfacial Electrochem. 317 (1991) 179.
[16] R. Prins, J. Chem. Soc. Chem. Commun. (1970) 280.
[17] A.B.P. Lever, Inorganic Electronic Spectroscopy, 2nd ed., Elsevier, Amsterdam, 1984.
[18] F. Hornung, F. Baumann, W. Kaim, J.A. Olabe, L.D. Slep, J. Fiedler, Inorg. Chem. 37 (1998) 311 and 5402.
[19] C. Elschenbroich, E. Bilger, R.D. Ernst, D.R. Wilson, M.S. Kralik, Organometallics 4 (1985) 2068.
[20] W. Kaim, S. Ernst, V. Kasack, J. Am. Chem. Soc. 112 (1990) 173.
[21] SHELXTLN, Version 5.1, Bruker AXS, 1998.